OPEN

Citation: Cell Death and Disease (2013) 4, e798; doi:10.1038/cddis.2013.306

www.nature.com/cddis

Preclinical screening of histone deacetylase inhibitors combined with ABT-737, rhTRAIL/MD5-1 or 5-azacytidine using syngeneic Vk*MYC multiple myeloma

GM Matthews*[,1,2], M Lefebure[1,2], MA Doyle[3], J Shortt[1,2], J Ellul[3], M Chesi[4], K-M Banks[1,2], E Vidacs[1,2], D Faulkner[5], P Atadja[6], PL Bergsagel[4] and RW Johnstone[1,2]

Multiple myeloma (MM) is an incurable malignancy with an unmet need for innovative treatment options. Histone deacetylase inhibitors (HDACi) are a new class of anticancer agent that have demonstrated activity in hematological malignancies. Here, we investigated the efficacy and safety of HDACi (vorinostat, panobinostat, romidepsin) and novel combination therapies using *in vitro* human MM cell lines and *in vivo* preclinical screening utilizing syngeneic transplanted Vk*MYC MM. HDACi were combined with ABT-737, which targets the intrinsic apoptosis pathway, recombinant human tumour necrosis factor-related apoptosis-inducing ligand (rhTRAIL/MD5-1), that activates the extrinsic apoptosis pathway or the DNA methyl transferase inhibitor 5-azacytidine. We demonstrate that *in vitro* cell line-based studies provide some insight into drug activity and combination therapies that synergistically kill MM cells; however, they do not always predict *in vivo* preclinical efficacy or toxicity. Importantly, utilizing transplanted Vk*MYC MM, we report that panobinostat and 5-azacytidine synergize to prolong the survival of tumor-bearing mice. In contrast, combined HDACi/rhTRAIL-based strategies, while efficacious, demonstrated on-target dose-limiting toxicities that precluded prolonged treatment. Taken together, our studies provide evidence that the transplanted Vk*MYC model of MM is a useful screening tool for anti-MM drugs and should aid in the prioritization of novel drug testing in the clinic.

Cell Death and Disease (2013) **4,** e798; doi:10.1038/cddis.2013.306; published online 12 September 2013
Subject Category: Cancer

Multiple myeloma (MM) is an incurable malignancy of plasma cells[1,2] characterized by clonal dysproteinemia, immune deregulation and end-organ toxicities associated with lytic bone destruction, renal failure, anemia and hypercalcemia.[3,4] Advances in the treatment of MM have been made recently;[5] however, many patients fail to respond or relapse after initial response, highlighting the requirement for novel agents and combination regimens.[6,7] Histone deacetylase inhibitors (HDACi) have demonstrated activity in hematological malignancies,[8–10] although resistance and dose-limiting toxicities are restricting their use.[11,12] Here, we evaluated the potential of augmenting antitumor activities of HDACi by their combination with agents targeting multiple apoptotic pathways or DNA methyltransferases. Preclinical evaluation of efficacy and associated toxicities of this approach were evaluated using the Vk*MYC model of MM.

Vorinostat (suborylanilide hydroxamic acid (SAHA)), an HDACi targeting multiple HDACs and romidepsin (depsipeptide), a class I-selective HDACi, are FDA approved for the treatment of cutaneous T-cell lymphoma.[13,14] Panobinostat (LBH-589), a cinnamic hydroxamic acid targeting multiple HDACs,[15] is undergoing phase III trials in combination with agents including bortezomib and dexamethasone in relapsed and refractory MM. HDACi induce apoptosis mainly via the intrinsic pathway[9] through events including altered cell cycle progression and/or cellular differentiation.[9,13,15–17] Hyperacetylation of non-histone proteins, including p53 and Hsp-90, may also have important roles in mediating antitumor effects of HDACi.[18] We posit that combining HDACi with agents targeting the intrinsic or extrinsic (death receptor) apoptotic pathways, or DNA-methyltransferases, could enhance therapeutic effects of HDACi[17] while reducing toxicities.

[1]Gene Regulation Laboratory, Cancer Therapeutics, Peter MacCallum Cancer Centre, St Andrews Place, East Melbourne, Victoria, Australia; [2]Sir Peter MacCallum Department of Oncology, University of Melbourne, East Melbourne, VIC, Australia; [3]Bioinformatics Core Facility, Peter MacCallum Cancer Centre, St Andrews Place, East Melbourne, VIC, Australia; [4]Comprehensive Cancer Centre and Laboratory Medicine and Pathology, Mayo Clinic Arizona, Scottsdale, AZ, USA; [5]Department of Pathology, Peter MacCallum Cancer Centre, St Andrews Place, East Melbourne, VIC, 3002, Australia and [6]Novartis Institutes for Biomedical Research, Cambridge, MA, USA

*Corresponding author: GM Matthews, Gene Regulation Laboratory, Cancer Therapeutics, Peter MacCallum Cancer Centre, St Andrews Place, East Melbourne, VIC 3002, Australia. Tel: +61 3 9656 3724; Fax: +61 3 9656 1411; E-mail: geoff.matthews@petermac.org

Keywords: multiple myeloma; histone deacetylase inhibitors; intrinsic apoptosis; extrinsic apoptosis; DNA methylation

Abbreviations: 5-AZA, 5-azacytidine; ANOVA, analysis of variance; BH3, Bcl-2 homology domain 3; CAMERA, correlation adjusted mean rank; c-FLIP, cytosolic Flice-like inhibitory protein; CI, combination index; DNMTi, DNA methyl transferase inhibitor; DR-4/5, death receptor-4/5; FDR, false discovery rate; HDAC, histone deacetylase; HDACi, histone deacetylase inhibitor; IP, intraperitoneal; JAK, Janus kinase; MGUS, monoclonal gammopathy of underdetermined significance; MM, multiple myeloma; rhTRAIL, recombinant human TNF-related apoptosis-inducing ligand; SAHA, suborylanilide hydroxamic acid; SPEP, serum protein electrophoresis; TNF, tumor necrosis factor; TRAIL, TNF-related apoptosis-inducing ligand

Received 18.12.12; revised 13.6.13; accepted 15.7.13; Edited by Y Shi

The intrinsic apoptotic pathway is regulated by prosurvival (e.g. Bcl-2, Bcl-X_L) and proapoptotic (e.g. Bax, Bak) multidomain Bcl-2 proteins, and Bcl-2 homology domain 3 (BH3)-only members.[19,20] ABT-737, a BH3-only mimetic that binds Bcl-2, Bcl-X_L and Bcl-w, acts by increasing the amount of free BH3-only proteins.[21–26] The death receptor pathway is stimulated by ligands from the tumor necrosis factor (TNF) family, including TNF-related apoptosis-inducing ligand (TRAIL), binding to death receptors DR-4 (TRAIL-R1) or DR-5 (TRAIL-R2)) on human cells, or DR-5 on murine cells.[27,28] Indeed, we have demonstrated that combining vorinostat with an agonistic anti-TRAIL receptor (TRAILR) antibody is more effective than single-agent treatment of breast cancer cell lines,[29,30] whereas ABT-737 resensitizes Bcl-2- and Bcl-X_L-overexpressing lymphoma cells to vorinostat.[31,32]

Recent work has demonstrated the potential for DNA methyltransferase inhibitors (DNMTi) in MM.[6,33] DNMTi reportedly induce apoptosis in MM cells through the down-regulation of Janus kinase-signal transducer and activator of transcription (JAK-STAT) signaling and nuclear factor-κB[6] and/or re-expression of epigenetically silenced genes, including tumor suppressors.[34] Promising preclinical data suggests that HDACi and DNMTi may synergize to induce apoptosis and tumor regression in MM.

The Vk*MYC transgenic mouse[3,35] represents the pathogenesis and clinical manifestations of human MM. It relies on the activation of MYC in plasma cells leading to histopathological and immunophenotypic features of human MM, including progression from monoclonal gammopathy of undetermined significance (MGUS) to end-organ destructive plasma cell expansion.[35] Chng *et al.*[36] demonstrated MYC activation for the progression of human MGUS to MM, highlighting biological relevance of the Vk*MYC model. Moreover, Chesi *et al.*[3,35] rigorously validated the ability of this model to predict single-agent drug activity in MM with a positive predictive value for clinical activity of 67% and a negative predictive value for clinical inactivity of 86%. Vk*MYC tumor cells are transplantable into syngeneic mice allowing for therapeutic experiments in large cohorts.[35]

Here, we investigated the potential of combining HDACi with ABT-737, recombinant human TNF-related apoptosis-inducing ligand (rhTRAIL)/MD5-1 or 5-azacytidine (5-AZA) in MM. We compared the effects of combination regimens *in vitro* in human MM cell lines with efficacy *in vivo* utilizing Vk*MYC MM. We demonstrate divergent effects of combination therapies *in vivo* compared with *in vitro* and identify toxicity profiles that only manifest in syngeneic model systems. We propose testing of new agents using Vk*MYC MM to aid in more rapid development of active and safe drug combinations for the treatment of MM.

Results

Differential sensitivities of human MM cell lines to HDACi. Human MM cell lines demonstrated differential time- and dose-dependent sensitivities to HDACi (Figure 1a). OPM-2 cells appeared most sensitive to vorinostat ($EC_{50} = 727$ nM; 48 h) compared with EC50s of 1828, 1896 and 2500 nM for JJN3, RPMI-8226 and U266 cells, respectively. JJN3 cells were the most sensitive line to panobinostat ($EC_{50} = 9$ nM; 48 h) compared with EC50s of 10, 35 and 16 nM for OPM-2, RPMI-8226 and U266 cells, respectively. JJN3 cells were most sensitive to romidepsin ($EC_{50} < 1$ nM; 48 h) compared with EC50s of 1, 1.8 and 10 nM for U266, RPMI-8226 and OPM-2 cells, respectively. To demonstrate the correlation between HDACi-mediated target inhibition and induction of apoptosis, pharmacodynamic analyses were performed using panobinostat as a reference HDACi using detection of histone-H3 acetylation as the readout. Figure 1b shows the dose-dependent acetylation of histone-H3 in each human cell line with panobinostat (0–50 nM; 24 h).

MM cell apoptosis is enhanced by combining HDACi with ABT-737. We have previously demonstrated that overexpression of prosurvival Bcl-2 proteins can inhibit HDACi-induced apoptosis.[31,32,37–39] We therefore determined whether relative sensitivities of MM cell lines to panobinostat were associated with the expression of Bcl-2 family members. Western blot analysis detected significant Bcl-2 expression in JJN3, OPM-2 and RPMI-8226, with barely detectable levels in U266 (Figure 2a). Bcl-X_L was detected in RPMI-8226 and U266, with little detected in JJN3 and OPM-2 cells. Mcl-1 was detected at high levels in all lines tested (Figure 2a), whereas Bcl-w and Bcl-A1 were undetectable (positive controls showed antibody specificity, data not shown). Assessment of microarray expression data sets (Oncomine) suggested that all cell lines expressed Bcl-2, Mcl-1 and low levels of Bcl-w, whereas the expression of Bcl-X_L and A1 correlated with protein levels by western blot (Supplementary Figure 1). Collectively, these data failed to demonstrate any direct correlation between HDACi sensitivity and expression of prosurvival Bcl-2 family proteins. Given that all four MM cell lines expressed high levels of Bcl-2 and/or Bcl-X_L, we assessed their sensitivity to ABT-737.[23,24] All four cell lines were sensitive to ABT-737, with the U266 line being slightly more resistant (Figure 2b).

Combining HDACi with ABT-737 kills B-cell lymphomas more potently than either agent alone,[31] and we therefore wished to determine the effect of this combination treatment against MM cells. The level of apoptosis following treatment of human MM cells with panobinostat and ABT-737 was significantly greater than single-agent treatment with a combination index (CI) < 0.9 demonstrating synergistic cell killing (Figure 2c and Supplementary Figures 2A–D). These studies indicate that combining HDACi with ABT-737 may be a potent method of killing MM cells.

Sensitivity of MM cells to the combination of HDACi and rhTRAIL. Previous studies have demonstrated that HDACi activate the extrinsic apoptosis pathway through the upregulation of death receptors (DR4 and DR5) and their cognate ligands (e.g. TRAIL).[29,30] We have shown that combining HDACi with agonistic anti-TRAIL receptor antibodies is effective in preclinical models of breast, colon and renal carcinoma.[17,30] *In vitro* sensitivity of cells to rhTRAIL correlated with surface TRAIL receptor expression (Figures 3a and b), with RPMI-8226 cells showing the highest expression of DR4 and DR5 and lowest apoptotic threshold

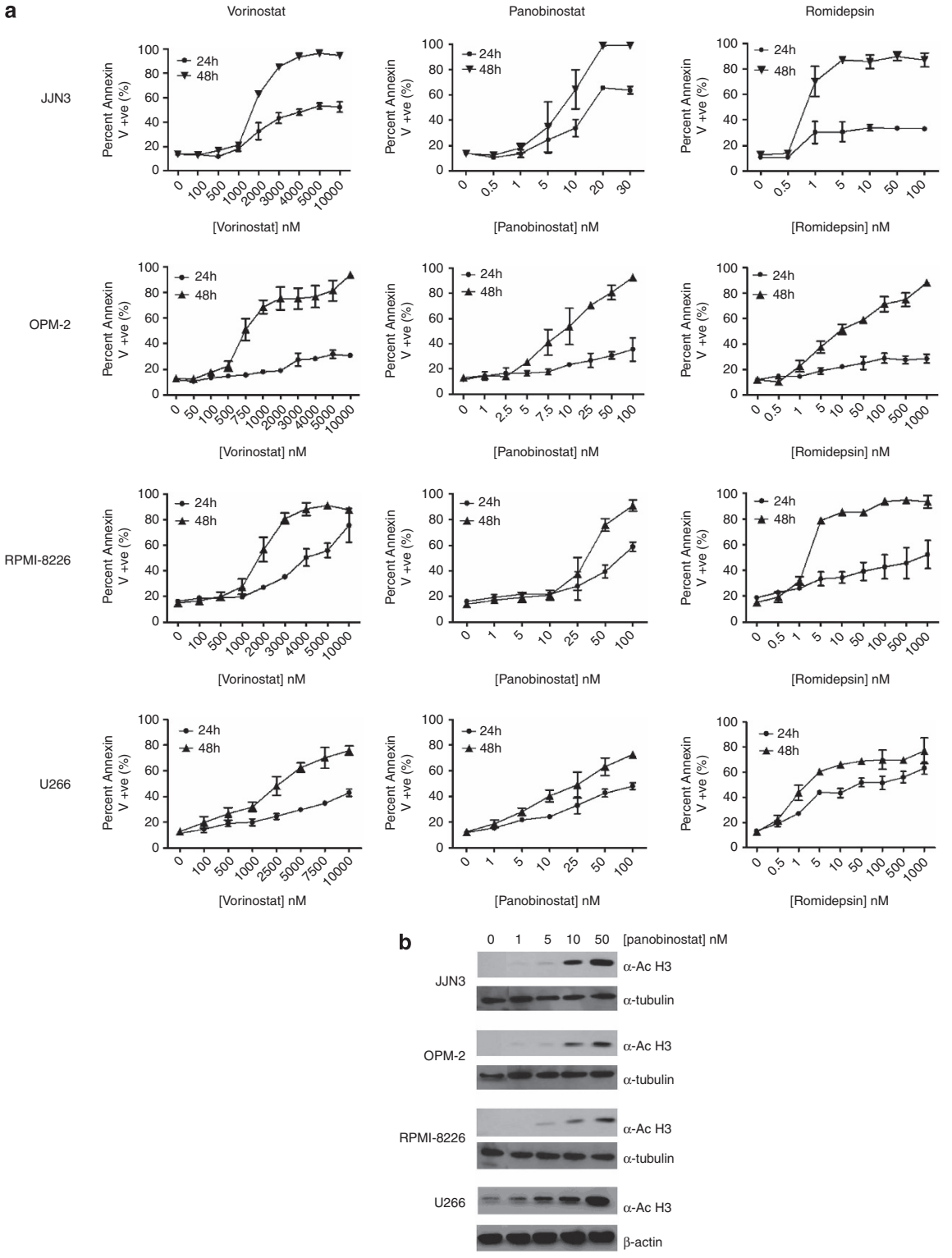

Figure 1 (**a**) Differential sensitivities of human MM cell lines to HDACi treatment. Single-agent dose–response curves constructed for each human MM cell line (JJN3, OPM-2, RPMI-8226 and U266) treated with vorinostat, panobinostat or romidepsin for 24 and 48 h. (**b**) On-target histone-H3 acetylation is demonstrated in a dose-dependent manner in human MM cell lines (JJN3, OPM-2, RPMI-8226 and U266) treated for 24 h with increasing doses of panobinostat (0, 1 5, 10 and 50 nM) and assessed by western blot

in response to TRAIL ($EC_{50} = 27$ ng/ml). For the other MM cell lines expressing low levels of DR-4/5, DR-4 expression was higher in the OPM-2 cell line and more closely correlated with rhTRAIL sensitivity ($EC_{50} = 60$ ng/ml; 48 h). Combining panobinostat with rhTRAIL synergistically induced apoptosis in RPMI-8226 and U266 cells. This combination induced

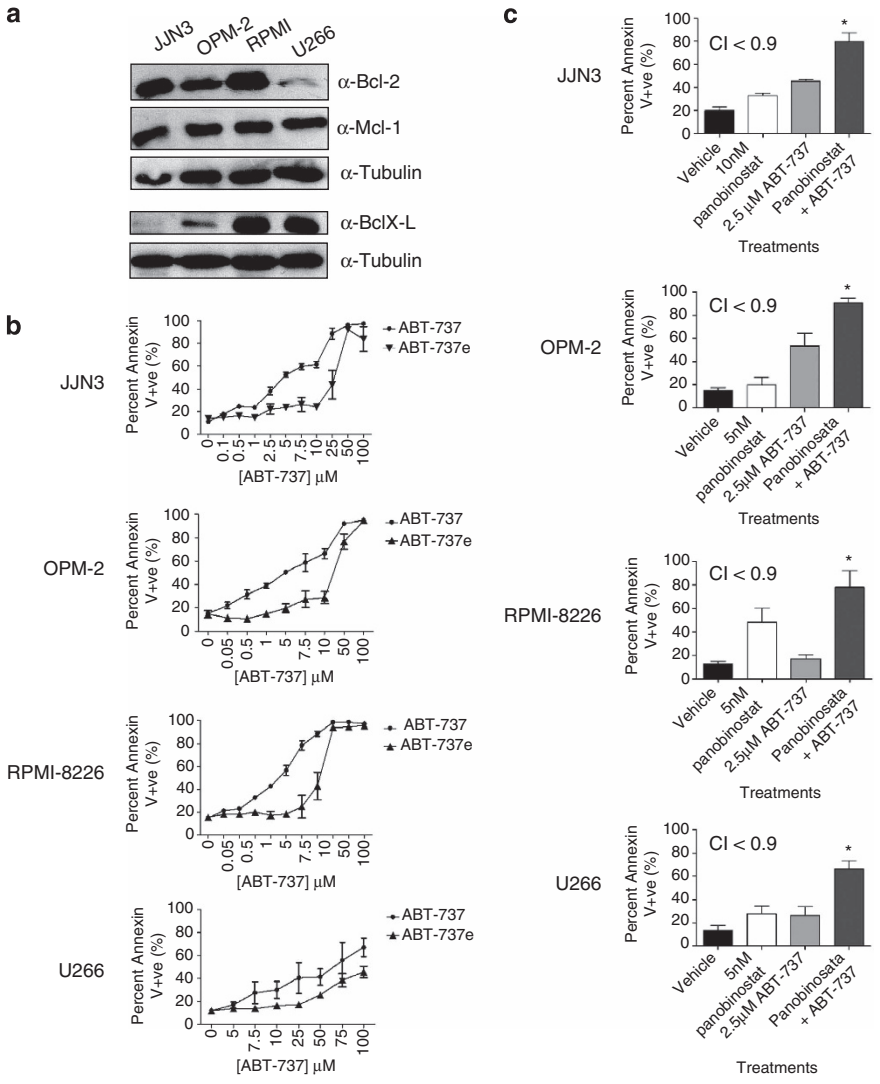

Figure 2 (**a**) Human MM cell lines demonstrate differential expression of Bcl-2 prosurvival proteins. JJN3, OPM-2, RPMI-8226 and U266 were assessed for the expression of antiapoptotic Bcl-2 proteins by western blot: Bcl-2, Bcl-X_L, Bcl-W, Mcl-1 and A1. (**b**) Differential sensitivities of human MM cell lines to ABT-737. Single-agent dose–response curves were constructed in human MM cell lines (JJN3, OPM-2, RPMI-8226 and U266) treated with ABT-737 for 24 and 48 h. (**c**) Synergistic induction of apoptosis in human MM cell lines JJN3, OPM-2, RPMI-8226 and U266 following 48 h treatment with panobinostat in combination with ABT-737 after 48 h incubation. $^*P < 0.05$ *versus* single agents. Calcusyn was used to determine synergy when the two agents were combined: synergy is determined when CI < 0.9, additively when CI is between 0.9 and 1.1 and antagonism when CI > 1.1. CI values are shown on each graph

additive levels of death in OPM-2 cells, whereas JJN3 cells remained relatively resistant to the combination (Figure 3c and Supplementary Figures 2E–H).

To elucidate mechanisms enabling HDACi to sensitize MM cells to rhTRAIL, panobinostat-treated cells were assessed for changes in cytosolic Flice-like inhibitory protein (c-$FLIP_L$) (Figures 3d and e) and DR-4/5 expression (Figure 3e). c-FLIP mRNA and protein expression (c-$FLIP_L$) was reduced in a cell- and dose-dependent manner in all MM cell lines following 8 or 16 h treatment (Figures 3d and e). Panobinostat increased DR-5 expression on RPMI-8226 cells but appeared to reduce DR-4 expression on U266 cells (Figure 3e). These data suggest that HDACi may sensitize MM cells to rhTRAIL-induced apoptosis by the upregulation of DR-5 and/or suppression of c-$FLIP_L$ in a cell- and dose-dependent manner.

MM cell apoptosis is enhanced by combining HDACi with 5-AZA. JJN3 and U266 cell lines with the highest and lowest sensitivity to panobinostat, respectively, were selected to investigate the potential for panobinostat to synergize with 5-AZA. JJN3 cells demonstrated dose-dependent sensitivities to 5-AZA treatment (Figure 4a) that synergized with panobinostat (Figure 4b and Supplementary Figures 2I–J) to induce rapid and robust cell death. U266 cells appeared relatively resistant to 5-AZA (Figure 4a); however, when combined with panobinostat, apoptosis increased greater than either agent alone (Figure 4b). RNA sequencing revealed significant changes (false discovery rate (FDR) < 0.05) to the expression of approximately 20%, 4% and 22% of analyzed genes (18 000) in JJN3 and 14%, 5% and 21% in U266 by panobinostat, 5-AZA or the

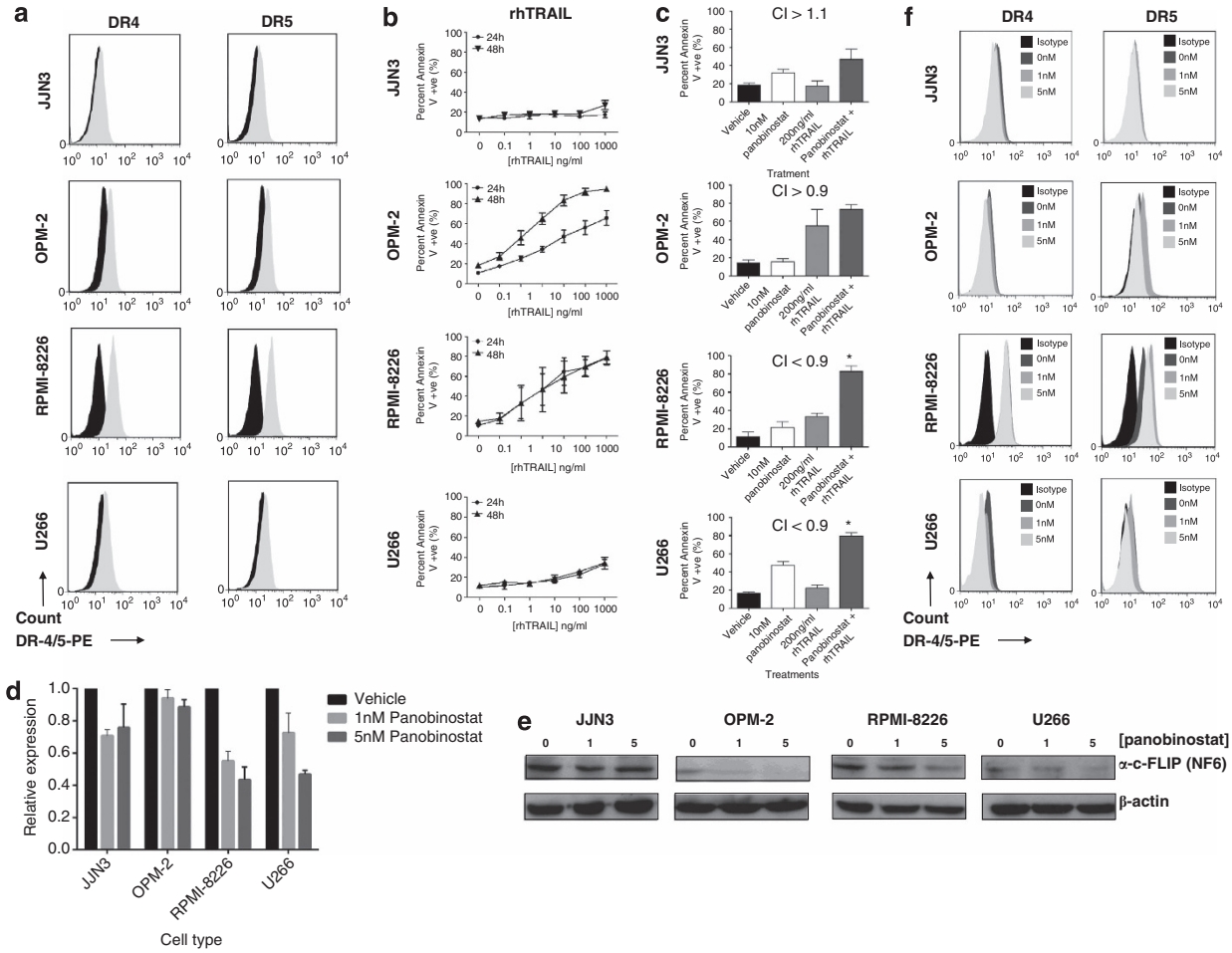

Figure 3 (**a**) Assessment of cell surface death receptor DR-4 and DR-5 on human MM cell lines JJN3, OPM-2, RPMI-8226 and U266, using flow cytometry against an isotype control antibody ($n=3$). Black histogram = isotype control; gray shaded histogram = DR4 or DR5 expression. (**b**) Differential sensitivities of human MM cell lines to rhTRAIL treatment. Single-agent dose–response curves were constructed in human MM cell lines (JJN3, OPM-2, RPMI-8226 and U266) treated with rhTRAIL for 24 and 48 h. (**c**) Synergistic induction of apoptosis in human MM cell lines OPM-2, RPMI-8226 and U266 following 48 h treatment with panobinostat and rhTRAIL (CI < 0.9). The combination of panobinostat with rhTRAIL did not synergize in JJN3 cells (CI > 1.1) and was only additive in OPM-2 cells (CI between 0.9 and 1.1). *$P<0.05$ *versus* single agents; analysis of c-FLIP (NF6) was undertaken in human MM cell lines (JJN3, OPM-2, RPMI-8226 and U266) following 8–16 h treatment with increasing doses of panobinostat below that shown to induce apoptosis (0, 1 and 5 nM). (**d**) Panobinostat significantly reduced c-FLIP mRNA expression levels in all cell types (8 h), whereas (**e**) protein expression was reduced in OPM-2, RPMI-8226 and U266 cells (16 h); and (**f**) assessment of cell surface DR-4/5 expression on human MM cell lines (JJN3, OPM-2, RPMI-8226 and U266) following treatment (16 h) with panobinostat ($n=3$). Panobinostat treatment significantly increased DR-5 expression on RPMI-8226 cells while appearing to reduce DR-4 expression on U266 cells ($P<0.05$). Black histogram = isotype control; dark gray shaded histogram = vehicle control; medium shade of gray histogram = 1 nM panobinostat; light shade of gray histogram = 5 nM panobinostat. At least $n=3$ biological replicates were carried out for each assessment

combination of both agents, respectively (data not shown). Specifically, panobinostat reproducibly lowered the transcription of IL-6, IL-6R and IL-6 signal transducer in both cell types, whereas 5-AZA reduced IL-6 transcription in U266 cells only. Combination treatment further reduced IL-6 in U266 cells only. Taken together, the reduced expression of IL-6 was not a common effect of combination therapy and unlikely to facilitate drug synergy in both cell lines.

Gene set enrichment analysis utilizing CAMERA (correlation adjusted mean rank)[40] revealed distinct molecular signatures when JJN3 and U266 cells were treated with combination therapies not seen during single-agent dosing (Figures 4c and d) (Tables 1a and b). We purport that the greater number of unique gene sets affected by combination therapy in JJN3 cells, which include relevant HDACi, methylation and MM signaling pathways may reflect the greater induction of apoptosis in this MM cell line than U266. In addition, we observed upregulation of a single gene set signature common to both cell lines that was unique to the combination therapy (Figure 4e and Table 1c). This suggests that activation of cell-line-specific molecular signatures may enable amplification of the synergistic apoptotic response when panobinostat and 5-AZA were combined.

Preclinical assessment of HDACi with ABT-737, MD5-1 or 5-AZA in Vk*MYC MM. We used the Vk*MYC model to test efficacy and tolerability of combining HDACi with ABT-737, MD5-1 an agonistic antibody against mouse DR-5 or 5-AZA. The expression of prosurvival Bcl-2 proteins and DR-5 was assessed by western blot and flow cytometry,

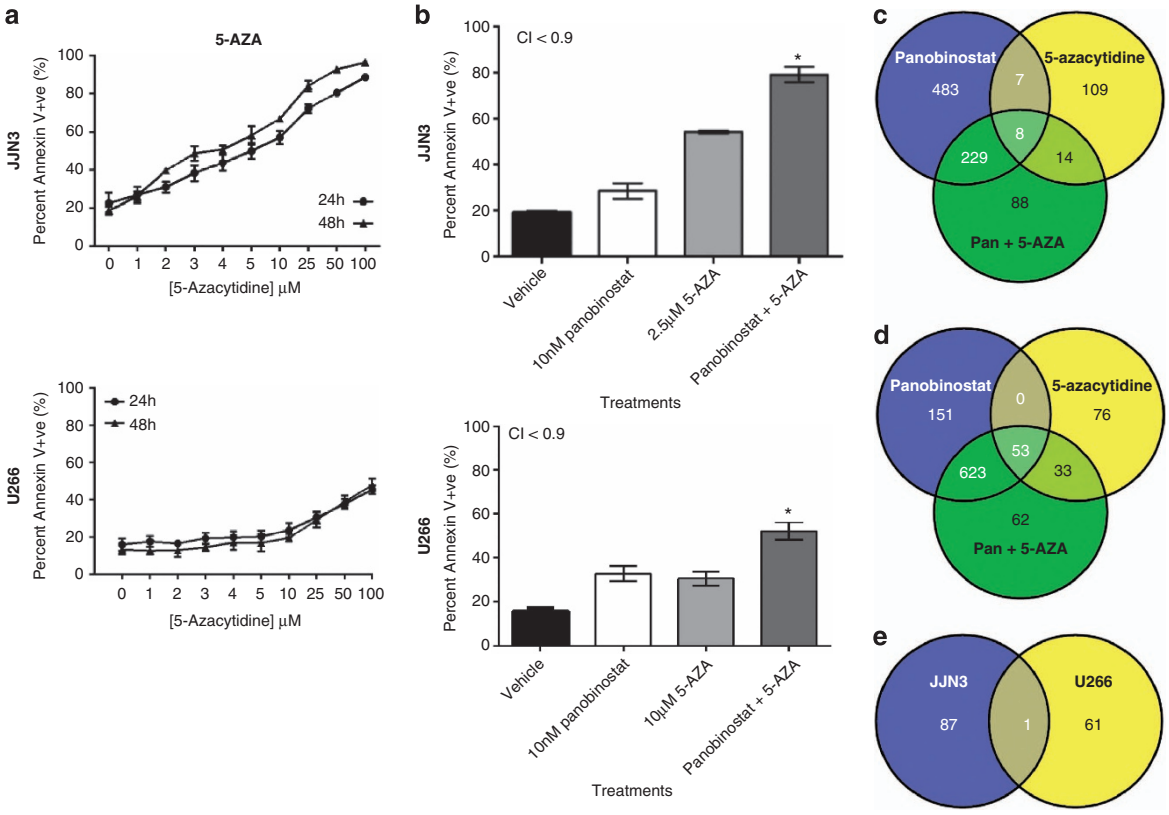

Figure 4 (**a**) Human MM cell lines display differential and dose-dependent sensitivities to 5-AZA. Single-agent dose–response curves were constructed in human MM cell lines (JJN3 and U266) treated with 5-AZA for 24 and 48 h. (**b**) Synergistic induction of apoptosis in JJN3 and U266 cells with panobinostat was combined with 5-AZA after 48 h (CI < 0.9) *$P < 0.05$ verses single agents: (**c**) JJN3 cells or (**d**) U266 cells were treated with panobinostat, 5-AZA or the combination of both agents at synergistic concentrations (described in Figure 4b) and assessed for changes in gene expression using next-generation RNA sequencing after 24 h. Gene set enrichment was assessed using CAMERA.[40] Each Venn diagram depicts the number of MSigDB gene sets enriched within each treatment and within each cell line (two-sided $P < 0.05$, $n = 3$); (**e**) demonstrates the number of distinct or overlapping MSigDB gene sets enriched when JJN3 or U266 cells were treated with the combination of panobinostat with 5-AZA

respectively (Figure 5). Primary Vk*MYC MM cells expressed Bcl-2, Bcl-X_L and Mcl-1 (Figure 5a) but not Bcl-w (data not shown), whereas FACS analysis confirmed the expression of mDR-5 on B220 − /CD138 + plasma cells (Figure 5b).

Mice bearing Vk*MYC tumor were treated with vehicle, panobinostat (25 mg/kg then 15 mg/kg), ABT-737 (75 mg/kg) or the combination of agents. This resulted in significant reductions in serum paraprotein over the period of therapy, resulting in a significant survival advantage in mice treated with panobinostat alone (median > 25 days) compared with vehicle control (median = 14 days, $P < 0.05$) (Figures 6a and b). In contrast, single-agent ABT-737 had neither effect on serum paraprotein nor the survival of mice bearing Vk*MYC MM (median = 11 days). Unfortunately, although serum paraprotein was significantly reduced (data not shown), the combination of panobinostat with ABT-737 led to all mice reaching end points by day 3 of treatment, putatively because of drug-induced toxicity (Figures 6a and b). Mice bearing Vk*MYC tumors were then treated with vehicle, low-dose panobinostat (5 mg/kg), ABT-737 (50 mg/kg) or the combination. The dose of panobinostat used was the maximum-tolerated dose when combined with ABT-737 (data not shown). Panobinostat significantly reduced paraprotein levels compared with vehicle-treated control levels (day 26, $P < 0.05$), whereas ABT-737 had no significant effect ($P > 0.05$) over the period of therapy (Figure 6c). Therefore, in contrast to *in vitro* data, combining both agents had no additional effect on serum paraprotein levels achieved by panobinostat treatment alone ($P > 0.05$) and no survival advantage was observed using the combination regimen (Figure 6d).

Mice bearing Vk*MYC tumor were treated with vehicle, panobinostat, MD5-1 and the combination. A significant reduction in serum paraprotein was observed after 5 days of panobinostat treatment, and further reduced in mice receiving combination treatment compared with vehicle controls (Figures 7a, $P < 0.05$). No change to serum paraprotein levels were observed with mice receiving MD5-1 treatment at this time ($P > 0.05$). Survival of mice receiving panobinostat alone was significantly increased compared with vehicle-treated mice (median = 40 *versus* 26.5 days, $P < 0.05$) (Figure 7b). In contrast, MD5-1-treated mice showed no survival benefit over mice treated with vehicle (median = 24 *versus* 26.5 days; $P > 0.05$), whereas all mice receiving combination therapy reached end points by day 10. These early deaths occurred in the combination treatment group despite significant reductions in tumor burden as assessed by reduction in serum paraprotein, indicating mortality due to drug toxicity

Table 1a Molecular signatures unique to the panobinostat and 5-AZA combination in JJN3 cells (Figure 4e)

Gene set	No. of genes	Direction	Two-sided *P*-value	FDR
JISON_SICKLE_CELL_DISEASE_DN	151	Down	0.006	0.491
CHEOK_RESPONSE_TO_MERCAPTOPURINE_DN	16	Up	0.003	0.491
SATO_SILENCED_BY_METHYLATION_IN_PANCREATIC_CANCER_2	30	Up	0.003	0.491
MIKKELSEN_IPS_HCP_WITH_H3_UNMETHYLATED	36	Up	0.012	0.491
KIM_RESPONSE_TO_TSA_AND_DECITABINE_UP	90	Up	0.016	0.491
MCGARVEY_SILENCED_BY_METHYLATION_IN_COLON_CANCER	25	Up	0.017	0.491
BIOCARTA_UCALPAIN_PATHWAY	16	Up	0.017	0.491
NUMATA_CSF3_SIGNALING_VIA_STAT3	17	Down	0.019	0.491
KIM_WT1_TARGETS_12 HR_DN	177	Down	0.019	0.491
KUNINGER_IGF1_VS_PDGFB_TARGETS_UP	47	Up	0.020	0.491
LABBE_TGFB1_TARGETS_UP	80	Up	0.020	0.491
SATO_SILENCED_EPIGENETICALLY_IN_PANCREATIC_CANCER	32	Up	0.021	0.491
APPEL_IMATINIB_RESPONSE	26	Up	0.021	0.491
LEE_LIVER_CANCER_CIPROFIBRATE_UP	37	Up	0.023	0.491
PID_ECADHERIN_KERATINOCYTE_PATHWAY	18	Up	0.025	0.491
REACTOME_TRAFFICKING_OF_AMPA_RECEPTORS	19	Up	0.026	0.491
KEGG_N_GLYCAN_BIOSYNTHESIS	44	Down	0.027	0.491
KUNINGER_IGF1_VS_PDGFB_TARGETS_DN	35	Up	0.027	0.491
ZHAN_MULTIPLE_MYELOMA_CD2_DN	45	Down	0.027	0.491
AIGNER_ZEB1_TARGETS	23	Up	0.028	0.491
REACTOME_CELL_JUNCTION_ORGANIZATION	54	Up	0.028	0.491
KEGG_TIGHT_JUNCTION	107	Up	0.029	0.491
VERRECCHIA_RESPONSE_TO_TGFB1_C2	24	Up	0.029	0.491
REACTOME_SEMA4D_IN_SEMAPHORIN_SIGNALING	29	Up	0.029	0.491
HELLER_SILENCED_BY_METHYLATION_UP	224	Up	0.029	0.491
BIOCARTA_FAS_PATHWAY	29	Down	0.030	0.491
REACTOME_G1_PHASE	35	Down	0.030	0.491
MEISSNER_BRAIN_HCP_WITH_H3K4ME2_AND_H3K27ME3	40	Up	0.030	0.491
PID_HIVNEFPATHWAY	32	Down	0.031	0.491
REACTOME_SEMA4D_INDUCED_CELL_MIGRATION_AND_GROWTH_CONE_COLLAPSE	25	Up	0.032	0.491
SHIN_B_CELL_LYMPHOMA_CLUSTER_2	27	Down	0.032	0.491
ZWANG_CLASS_2_TRANSIENTLY_INDUCED_BY_EGF	34	Up	0.032	0.491
JOHANSSON_GLIOMAGENESIS_BY_PDGFB_DN	18	Up	0.033	0.491
REACTOME_STRIATED_MUSCLE_CONTRACTION	18	Up	0.034	0.491
LIANG_SILENCED_BY_METHYLATION_2	35	Up	0.034	0.491
BIOCARTA_ARF_PATHWAY	17	Down	0.034	0.491
BACOLOD_RESISTANCE_TO_ALKYLATING_AGENTS_UP	20	Up	0.034	0.491
CREIGHTON_ENDOCRINE_THERAPY_RESISTANCE_2	389	Up	0.035	0.491
REACTOME_CELL_CELL_COMMUNICATION	87	Up	0.035	0.491
REACTOME_AXON_GUIDANCE	207	Up	0.035	0.491
BRACHAT_RESPONSE_TO_METHOTREXATE_UP	23	Up	0.035	0.491
RAMPON_ENRICHED_LEARNING_ENVIRONMENT_LATE_UP	19	Down	0.036	0.491
MIPS_28S_RIBOSOMAL_SUBUNIT_MITOCHONDRIAL	30	Down	0.036	0.491
KEGG_FOCAL_ADHESION	168	Up	0.036	0.491
REACTOME_RECYCLING_PATHWAY_OF_L1	26	Up	0.037	0.491
HAHTOLA_MYCOSIS_FUNGOIDES_CD4_DN	112	Down	0.037	0.491
MCBRYAN_PUBERTAL_TGFB1_TARGETS_DN	41	Up	0.038	0.491
CLASPER_LYMPHATIC_VESSELS_DURING_METASTASIS_UP	16	Up	0.038	0.491
MATZUK_SPERMATOZOA	81	Up	0.038	0.491
MARTENS_TRETINOIN_RESPONSE_UP	377	Up	0.038	0.491
MOREAUX_B_LYMPHOCYTE_MATURATION_BY_TACI_UP	70	Up	0.039	0.491
DORSEY_GAB2_TARGETS	22	Up	0.039	0.491
LIAN_LIPA_TARGETS_6M	34	Up	0.039	0.491
VANTVEER_BREAST_CANCER_BRCA1_UP	32	Down	0.040	0.491
MISSIAGLIA_REGULATED_BY_METHYLATION_UP	102	Up	0.041	0.491
MIPS_55S_RIBOSOME_MITOCHONDRIAL	77	Down	0.041	0.491
VALK_AML_CLUSTER_15	23	Up	0.042	0.491
REACTOME_MITOCHONDRIAL_TRNA_AMINOACYLATION	20	Down	0.042	0.491
CHIANG_LIVER_CANCER_SUBCLASS_POLYSOMY7_UP	55	Up	0.042	0.491
SATO_SILENCED_BY_METHYLATION_IN_PANCREATIC_CANCER_1	286	Up	0.042	0.491
BIOCARTA_AGR_PATHWAY	27	Up	0.042	0.491
CROONQUIST_STROMAL_STIMULATION_UP	45	Up	0.043	0.491
NIELSEN_SYNOVIAL_SARCOMA_UP	15	Up	0.043	0.491
HUANG_GATA2_TARGETS_DN	62	Down	0.043	0.491
KEGG_LEUKOCYTE_TRANSENDOTHELIAL_MIGRATION	91	Up	0.044	0.491
ONKEN_UVEAL_MELANOMA_UP	731	Down	0.045	0.491
PID_S1P_S1P1_PATHWAY	19	Up	0.045	0.491
YAO_TEMPORAL_RESPONSE_TO_PROGESTERONE_CLUSTER_1	59	Up	0.045	0.491
ZHANG_TLX_TARGETS_DN	91	Up	0.046	0.491
GU_PDEF_TARGETS_DN	25	Up	0.046	0.491
ZHONG_RESPONSE_TO_AZACITIDINE_AND_TSA_DN	64	Down	0.047	0.491
VILIMAS_NOTCH1_TARGETS_UP	39	Up	0.047	0.491

Table 1a *(Continued)*

Gene set	No. of genes	Direction	Two-sided *P*-value	FDR
BURTON_ADIPOGENESIS_7	41	Up	0.047	0.491
PID_INTEGRIN_A9B1_PATHWAY	17	Up	0.047	0.491
REACTOME_CELL_SURFACE_INTERACTIONS_AT_THE_VASCULAR_WALL	62	Up	0.048	0.491
ZHONG_RESPONSE_TO_AZACITIDINE_AND_TSA_UP	162	Up	0.048	0.491
BAELDE_DIABETIC_NEPHROPATHY_UP	56	Up	0.048	0.491
MULLIGAN_NTF3_SIGNALING_VIA_INSR_AND_IGF1R_UP	18	Down	0.048	0.491
BRACHAT_RESPONSE_TO_CAMPTOTHECIN_UP	26	Up	0.049	0.491
REACTOME_NEF_MEDIATES_DOWN_MODULATION_OF_CELL_SURFACE_RECEPTORS_BY_RECRUITING_THEM_TO_CLATHRIN_ADAPTERS	16	Up	0.049	0.491
POTTI_CYTOXAN_SENSITIVITY	30	Up	0.049	0.491
GOLUB_ALL_VS_AML_DN	18	Up	0.049	0.491
MIPS_39S_RIBOSOMAL_SUBUNIT_MITOCHONDRIAL	47	Down	0.049	0.491
KIM_MYC_AMPLIFICATION_TARGETS_UP	169	Down	0.049	0.491
LIN_SILENCED_BY_TUMOR_MICROENVIRONMENT	67	Up	0.049	0.491
PID_THROMBIN_PAR1_PATHWAY	37	Up	0.049	0.491
CHIANG_LIVER_CANCER_SUBCLASS_INTERFERON_DN	42	Up	0.049	0.491

CAMERA results for the gene sets from the MSigDB from panobinostat- and 5-AZA-treated JJN3 cells. Data include the size of each set, direction of gene set alterations, two-sided *P*-value and FDR

rather than disease progression. In an attempt to overcome the toxicities observed, the dose of panobinostat was reduced. Treatment with panobinostat alone (7.5 mg/kg) led to significant reductions in serum paraprotein ($P<0.05$), whereas MD5-1 alone, and its combination with panobinostat, had no significant effect ($P>0.05$) (Figure 7c). Treatment with panobinostat resulted in an increase in survival of tumor-bearing mice compared with vehicle treatment (median = 18 *versus* 39 days, $P<0.05$), whereas MD5-1 had a marginal effect on mouse survival (median = 18 *versus* 25 days, $P>0.05$) (Figure 7d). Interestingly, even with the reduced dosage of panobinostat, combination treatment with MD5-1 was still intolerable with mice succumbing earlier than vehicle-treated mice (median = 18 *versus* 15 days, $P>0.05$) (Figure 7d). Similar toxicities using the combination of panobinostat and MD5-1 were observed in mice bearing a second independently derived Vk*MYC myeloma (data not shown).

To determine whether the toxicity of combined panobinostat/MD5-1 treatment was due to direct effects on host cells, the experiment was repeated using C57BL/6.DR5$^{-/-}$ mice bearing transplanted Vk*MYC tumor. Mice were treated with vehicle, panobinostat (7.5 mg/kg), MD5-1 (50 μg per mouse) and the combination of both agents. In contrast to experiments in wild-type mice, no dose-limiting toxicity was observed (Figure 7e). As shown previously, MD5-1 treatment alone had no effect on survival compared with control-treated mice (median = 27.5 *versus* 30.5 days, $P>0.05$), whereas panobinostat alone significantly increased the median survival time (median = 39.5 days, $P<0.05$). Remarkably, in the absence of on-target toxicity, the combination of panobinostat and MD5-1 provided the greatest survival advantage in tumor-bearing C57BL/6.DR5$^{-/-}$ mice with a significant increase in survival compared with vehicle-treated mice (median = 54 *versus* 30.5 days; $P<0.05$) (Figure 7e).

Finally, mice bearing Vk*MYC tumor were treated with vehicle, panobinostat, 5-AZA or the combination. After 12 days of treatment, a significant reduction in serum paraprotein was observed in panobinostat- and 5-AZA-treated mice that were further reduced when the two agents were combined (Figure 7f). Importantly, the combination of panobinostat with 5-AZA led to the greatest survival advantage in tumor-bearing mice over vehicle-treated mice, greater than doubling their survival time (median = 32 *versus* 68.5 days; $P<0.05$) (Figure 7g).

Discussion

MM is an incurable malignancy with an unmet need for novel therapeutic agents.[5] Here, we combined *in vitro* cell line-based profiling with *in vivo* pre-clinical screening utilizing syngeneic transplanted Vk*MYC MM to investigate efficacy and safety of single-agent and combination therapies. HDACi were the primary agents under investigation and these were combined with ABT-737 targeting the intrinsic apoptosis pathway; rhTRAIL/MD5-1 that activates the extrinsic pathway or the DNMTi 5-AZA. We demonstrate that while *in vitro* studies provide some insight into drug combinations that synergistically kill MM cells, they do not guarantee their efficacy or tolerability *in vivo*. Our results provide evidence that Vk*MYC MM may aid in predicting clinical utilization of novel therapies by eliminating ineffective drug combinations and identifying associated on-target toxicities. Moreover, we describe the potential for HDACi to synergize with agents inhibiting DNA methylation, such as 5-AZA, in MM.

Recent investigations have highlighted the potential for HDACi in the treatment of MM.[41,42] Indeed, the Vk*MYC model has proven useful in predicting that the combination of HDACi with bortezomib would be safe and effective for the treatment of MM.[35] Here, we demonstrated the induction of apoptosis in four human MM cell lines by vorinostat, panobinostat and romidepsin concomitant with on-target histone H3 acetylation. Owing to the low nanomolar activity of panobinostat *in vitro* and current phase III testing, this pan-HDACi was utilized in all further single-agent and combination experiments.

Previous investigators have suggested that the expression of prosurvival Bcl-2 family proteins can determine HDACi

Table 1b Molecular signatures unique to the panobinostat and 5-AZA combination in U266 cells (Figure 4e)

Gene Set	No. of genes	Direction	Two-sided *P*-value	FDR
KRASNOSELSKAYA_ILF3_TARGETS_DN	39	Down	0.011	0.168
ISHIDA_E2F_TARGETS	52	Down	0.014	0.170
WU_APOPTOSIS_BY_CDKN1A_VIA_TP53	53	Down	0.016	0.172
CHEMNITZ_RESPONSE_TO_PROSTAGLANDIN_E2_UP	135	Down	0.018	0.179
REACTOME_MEIOSIS	61	Down	0.023	0.182
NUNODA_RESPONSE_TO_DASATINIB_IMATINIB_UP	29	Down	0.025	0.186
RUIZ_TNC_TARGETS_DN	131	Down	0.026	0.190
BIOCARTA_NOS1_PATHWAY	15	Up	0.027	0.191
BLUM_RESPONSE_TO_SALIRASIB_DN	325	Down	0.028	0.193
YU_BAP1_TARGETS	28	Down	0.028	0.193
BERTUCCI_INVASIVE_CARCINOMA_DUCTAL_VS_LOBULAR_DN	26	Up	0.029	0.197
REACTOME_ACTIVATION_OF_NMDA_RECEPTOR_UPON_GLUTAMATE_BINDING_AND_POSTSYNAPTIC_EVENTS	25	Up	0.031	0.201
MARTENS_TRETINOIN_RESPONSE_DN	682	Down	0.032	0.202
REACTOME_FANCONI_ANEMIA_PATHWAY	20	Down	0.033	0.203
REACTOME_ACTIVATION_OF_THE_PRE_REPLICATIVE_COMPLEX	28	Down	0.033	0.204
REACTOME_CREB_PHOSPHORYLATION_THROUGH_THE_ACTIVATION_OF_RAS	19	Up	0.033	0.204
REACTOME_DNA_STRAND_ELONGATION	29	Down	0.034	0.205
KORKOLA_EMBRYONIC_CARCINOMA_VS_SEMINOMA_DN	18	Up	0.035	0.206
KYNG_WERNER_SYNDROM_UP	20	Up	0.035	0.206
NOUSHMEHR_GBM_SILENCED_BY_METHYLATION	36	Up	0.036	0.209
REACTOME_DEPOSITION_OF_NEW_CENPA_CONTAINING_NUCLEOSOMES_AT_THE_CENTROMERE	35	Down	0.036	0.209
NIELSEN_LIPOSARCOMA_DN	17	Up	0.037	0.209
REACTOME_HOMOLOGOUS_RECOMBINATION_REPAIR_OF_REPLICATION_INDEPENDENT_DOUBLE_STRAND_BREAKS	16	Down	0.037	0.209
REACTOME_POST_NMDA_RECEPTOR_ACTIVATION_EVENTS	24	Up	0.037	0.209
MAHAJAN_RESPONSE_TO_IL1A_DN	63	Up	0.038	0.210
KEGG_MELANOGENESIS	74	Up	0.040	0.216
KEGG_ALDOSTERONE_REGULATED_SODIUM_REABSORPTION	34	Up	0.040	0.216
JAZAERI_BREAST_CANCER_BRCA1_VS_BRCA2_DN	38	Up	0.041	0.217
ST_T_CELL_SIGNAL_TRANSDUCTION	38	Down	0.041	0.217
LUI_THYROID_CANCER_CLUSTER_1	49	Up	0.041	0.218
GARGALOVIC_RESPONSE_TO_OXIDIZED_PHOSPHOLIPIDS_TURQUOISE_DN	53	Down	0.042	0.221
IVANOVA_HEMATOPOIESIS_STEM_CELL	205	Up	0.043	0.222
BENPORATH_ES_2	29	Down	0.043	0.222
REACTOME_LAGGING_STRAND_SYNTHESIS	18	Down	0.043	0.223
REACTOME_SYNTHESIS_OF_PC	16	Up	0.043	0.223
WAMUNYOKOLI_OVARIAN_CANCER_GRADES_1_2_DN	53	Up	0.044	0.224
LINDGREN_BLADDER_CANCER_CLUSTER_3_UP	307	Down	0.044	0.225
REACTOME_EXTENSION_OF_TELOMERES	25	Down	0.045	0.226
LINDGREN_BLADDER_CANCER_CLUSTER_1_DN	336	Down	0.045	0.226
AUNG_GASTRIC_CANCER	39	Down	0.045	0.227
CASORELLI_APL_SECONDARY_VS_DE_NOVO_UP	34	Up	0.045	0.227
KEGG_BASE_EXCISION_REPAIR	32	Down	0.045	0.227
PID_WNT_NONCANONICAL_PATHWAY	30	Up	0.046	0.227
TONKS_TARGETS_OF_RUNX1_RUNX1T1_FUSION_GRANULOCYTE_UP	46	Up	0.046	0.227
PID_SYNDECAN_2_PATHWAY	25	Up	0.046	0.227
STAEGE_EWING_FAMILY_TUMOR	21	Up	0.046	0.227
REACTOME_SIGNALING_BY_NOTCH1	66	Up	0.046	0.227
CHANG_IMMORTALIZED_BY_HPV31_UP	63	Up	0.046	0.227
REACTOME_PYRIMIDINE_METABOLISM	18	Down	0.046	0.227
PAL_PRMT5_TARGETS_UP	187	Down	0.046	0.227
REACTOME_MEIOTIC_RECOMBINATION	36	Down	0.047	0.228
BIOCARTA_CELLCYCLE_PATHWAY	23	Down	0.048	0.228
KEGG_FC_GAMMA_R_MEDIATED_PHAGOCYTOSIS	85	Up	0.048	0.229
CHICAS_RB1_TARGETS_LOW_SERUM	86	Down	0.048	0.229
SPIELMAN_LYMPHOBLAST_EUROPEAN_VS_ASIAN_UP	451	Down	0.048	0.229
REACTOME_RECRUITMENT_OF_MITOTIC_CENTROSOME_PROTEINS_AND_COMPLEXES	63	Down	0.049	0.231
KEGG_WNT_SIGNALING_PATHWAY	123	Up	0.049	0.231
HELLER_HDAC_TARGETS_DN	279	Down	0.049	0.231
REACTOME_GLYCEROPHOSPHOLIPID_BIOSYNTHESIS	69	Up	0.049	0.231
SESTO_RESPONSE_TO_UV_C8	66	Up	0.049	0.231
RODRIGUES_THYROID_CARCINOMA_UP	15	Down	0.049	0.232

CAMERA results for the gene sets from the MSigDB from panobinostat- and 5-AZA-treated U266 cells. Data include the size of each set, direction of gene set alterations, two-sided *P*-value and FDR

sensitivity.[38,43,44] Therefore, we assessed Bcl-2, Bcl-X_L, Bcl-w, Mcl-1 and A1. Bcl-2 and Bcl-X_L expression levels were varied, whereas high levels of Mcl-1 remained relatively constant between cell lines (Bcl-w and A1 were not detected). This suggests that expression of Bcl-2 family proteins does not adequately predict sensitivity to panobinostat within

Table 1c Molecular signature unique to the panobinostat and 5-azacytidine combination and common to JJN3 and U266 cells (Figure 4e)

Gene set	No. of genes	Direction	Two-sided *P*-value	FDR
REACTOME_L1CAM_INTERACTIONS	72	Up	0.015	0.491
		Up	0.048	0.228

Overlapping CAMERA results for the gene sets from the MSigDB from panobinostat- and 5-AZA-treated JJN3 (top) and U266 (bottom) cells. Data include the size of each set, direction of gene set alterations, two-sided *P*-value and FDR

this study. However, expression of Bcl-2 and Bcl-X_L in these MM cells provided a molecular rationale for testing the ability of ABT-737 to synergize with panobinostat. Combining panobinostat with ABT-737 over a broad concentration range resulted in significant induction of apoptosis in all MM cell lines tested. The level of apoptosis induced was more than additive and most likely due to concomitant activation of the intrinsic death pathway by both agents.[16,25] These *in vitro* results suggested the potential for this drug combination in treating MM.

A second therapy investigated, combining panobinostat with rhTRAIL, was based on the significant expression of death receptors DR-4 and DR-5 on two of the human MM cell lines tested. Previous investigators have documented the sensitivity of various MM cell lines to TRAIL-induced cell death, and the capability of HDACi to synergize with rhTRAIL through mechanisms including reactivation of silenced caspase-8,[12] downregulation of c-FLIP[12,27,45–47] and restoration of cell surface DR-4/5 expression.[48] We demonstrated synergistic induction of apoptosis in OPM-2 and RPMI-8226 cells when panobinostat was combined with rhTRAIL. This marked synergism was also detected in U266 cells, which express very low levels of DR-4/5 and are insensitive to single-agent rhTRAIL. Furthermore, we observed that panobinostat treatment increased surface DR-5 expression and loss of c-$FLIP_L$ in a cell line-dependent manner.

Previous studies investigating appropriate drug combinations for the treatment of MM have utilized human xenografts and immunodeficient mice.[26,49,50] The Vk*MYC model faithfully mimics human MM and provides a physiologically relevant tool for preclinical screening of novel therapeutics.[3,35] Transplanted Vk*MYC MM enables testing of therapeutics in younger mice without the time and expense involved in aging *de novo* Vk*MYC mice. Utilizing wild-type C57BL/6 mice bearing Vk*MYC tumor cells, we demonstrated that although *in vitro* cell culture studies suggest that a drug combination might be effective, these *in vitro* studies do not always translate *in vivo*. As an example, while combined panobinostat and ABT-737 induced synergistic death of human MM cell lines *in vitro*, the combination was too toxic and provided no significant survival benefit over panobinostat alone when tested at the MTD *in vivo*. This is considering a large reduction in paraprotein levels detected in combination treated mice (day 3, data not shown). It is important to consider the biological consequences of interactions between MM cells and the microenvironment within the bone marrow niche that may protect against ABT-737-induced apoptosis. Indeed, ABT-737 and its analog ABT-263 show reduced efficacy against nodally based CLL cells compared with circulating disease.[51,52] This might explain the divergent efficacy of ABT-737 against MM cell lines tested *in vitro* compared with Vk*MYC MM cells resident in the transplanted host.

In contrast to the effects of ABT-737, the agonistic anti-DR5 monoclonal antibody MD5-1 synergized with HDACi to kill human MM cell lines *in vitro* and induce myeloma regressions *in vivo*. However, this was achieved at the expense of prohibitive on-target *in vivo* toxicity conferred by the combination regimen. Importantly, the efficacy of combined panobinostat and MD5-1 could be maintained in the absence of toxicity in DR-5 knockout recipient mice in agreement with our previous studies.[17] Therefore, combined rhTRAIL/HDACi-based strategies may be used to overcome MM drug resistance in the human setting, if dose-limiting toxicities can be managed.

Profiling drug combinations using *in vitro* cell line-based investigations and Vk*MYC MM highlighted synergy when panobinostat is combined with 5-AZA. RNA sequencing of human MM cell lines JJN3 and U266 highlight distinct molecular signatures that may explain the potent cell line-dependent synergies seen when the two agents are combined. Importantly, our results suggest that targeting the epigenome through two molecularly distinct mechanisms, by coadministration of HDACi and DNMTi, has the ability to enhance the sensitivity of MM cells to apoptosis induction, leading to greater survival in mice bearing Vk*MYC MM.

These comprehensive studies into combination therapies consisting of panobinostat with ABT-737, rhTRAIL/MD5-1 or 5-AZA demonstrate the potential for Vk*MYC MM as a preclinical screening tool. In line with our recent publication,[35] we clearly demonstrate that panobinostat treatment provides a significant survival advantage with even relatively low dosages of drug. Importantly, the use of Vk*MYC MM allowed us to document the lack of activity of ABT-737 when combined with panobinostat and identify a toxicity profile observed following combination of panobinostat with MD5-1 that restricts efficacious dosing of this dual treatment regimen. Remarkably, we report the synergistic induction of apoptosis *in vitro* when panobinostat is combined with 5-AZA that is demonstrated by significant reductions to tumor load *in vivo* and increased survival advantage. These studies provide evidence that Vk*MYC MM is a useful screening tool for anti-MM drugs and should aid in prioritization of novel drug testing in the clinic.

Materials and Methods

Cells, chemicals and antibodies. JJN3 cells were a gift from Andrew Spencer (The Alfred Hospital, Prahran, VIC, Australia). RPMI-8226, OPM-2 and U266 cells were a gift from Paul Neeson (Hematology and Immunology Translational Research Laboratory, Peter MacCallum Cancer Centre, East Melbourne, VIC, Australia). JJN3 cells were cultured in the medium containing 40% IMDM, 40% DMEM, 20% FBS; OPM-2 and RPMI-8226 cells were cultured in

RPMI 1640 containing 10% FBS and L-glutamine; U266 cells were cultured in RPMI 1640 plus 15% FBS, sodium pyruvate, HEPES and L-glutamine. All cells were cultured with penicillin/streptomycin. Vorinostat (suberoylanilide hydroxamic acid, SAHA) was obtained from Merck (Boston, MA, USA), panobinostat (LBH-589) was obtained from Novartis Institutes for Biomedical Research (Cambridge, MA, USA), and romidepsin (Depsipeptide) and 5-AZA (Vidaza) were obtained from Celgene (Summit, NJ, USA). ABT-737 and ABT-737 enantiomer were obtained from Abbott (Abbot Park, IL, USA). rhTRAIL was obtained from Peprotech (Rocky Hill, NJ, USA). MD5-1 agonistic anti-mouse TRAILR Ab and control hamster mAb (UC8-1B9) were obtained from Hideo Yagita (Juntendo University School of Medicine, Tokyo, Japan). Western blotting antibodies included: anti-acetylated histone H3 (Millipore, Billerica, MA, USA); anti-hBcl-2 (SantaCruz Biotechnology, SantaCruz, CA, USA); anti-mBcl-2 (BD Pharmingen, North Ryde, NSW, Australia), anti-hBcl-xL (BD Pharmingen); anti-Mcl-1 (BD Pharmingen); anti-Bcl2-A1 (J Borst, The Netherlands Cancer Institute, Amsterdam, The Netherlands); anti-Bcl-w (16H12, Millipore); anti-hDR-4 and -hDR-5 (Imgenex, San Diego, CA, USA); anti-mDR-5 (BD Pharmingen); and anti-cFLIP$_L$ NF6 (Alexis, Sapphire Biosciences, Waterloo, NSW, Australia).

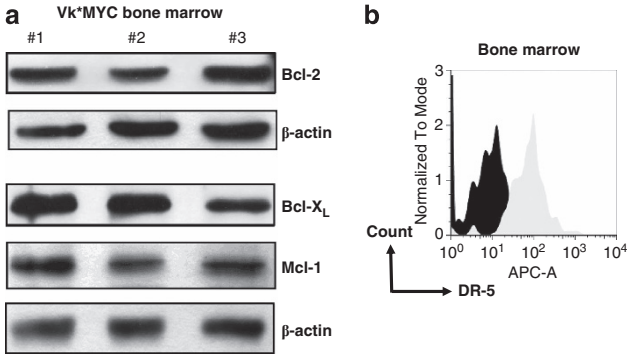

Figure 5 Expression of Bcl-2 prosurvival proteins and surface DR-5 on bone marrow cells from C57BL/6 mice bearing Vk*MYC MM. (**a**) Prosurvival Bcl-2 family protein expression in the bone marrow of mice bearing Vk*MYC MM by western blot ($n=3$), and (**b**) assessment of surface DR-5 expression on B220 − /CD138 + plasma cells from bone marrow of a mouse bearing Vk*MYC MM by FACS. Black histogram = isotype control; light gray histogram = DR-5 expression

***In vitro* apoptosis.** Cells seeded (2–5 × 10^5 per well) into 24-well plates (750 μl) were treated with vorinostat, panobinostat, romidesin, ABT-737, rhTRAIL or 5-AZA (750 μl). For combination studies, MM cell lines were treated with panobinostat and ABT-737, rhTRAIL or 5-AZA in a checkerboard format: vehicle (750 μl medium); single agent for each drug (375 μl drug + 375 μl medium); and combination drug treatments (375 μl drug A + 375 μl drug B). For combination treatments consisting of panobinostat and 5-AZA, cells were pretreated with 5-AZA for 24 h before the addition of panobinostat. Apoptosis (24 and 48 h) was assessed by FACS (Canto II; Becton Dickinson, Scoresby, VIC, Australia) using Annexin V-FITC and propidium iodide (PI) and results analyzed using the FlowJo software (version 7.6.5; Treestar, Ashland, OR, USA) and presented as the percentage of Annexin V-positive cells from at least three individual experiments.

Western blotting and quantitative real-time polymerase chain reaction. Cells seeded in six-well plates were treated with each agent for 8, 16 or 24 h, before freezing at − 80 °C. For protein expression by western blotting,

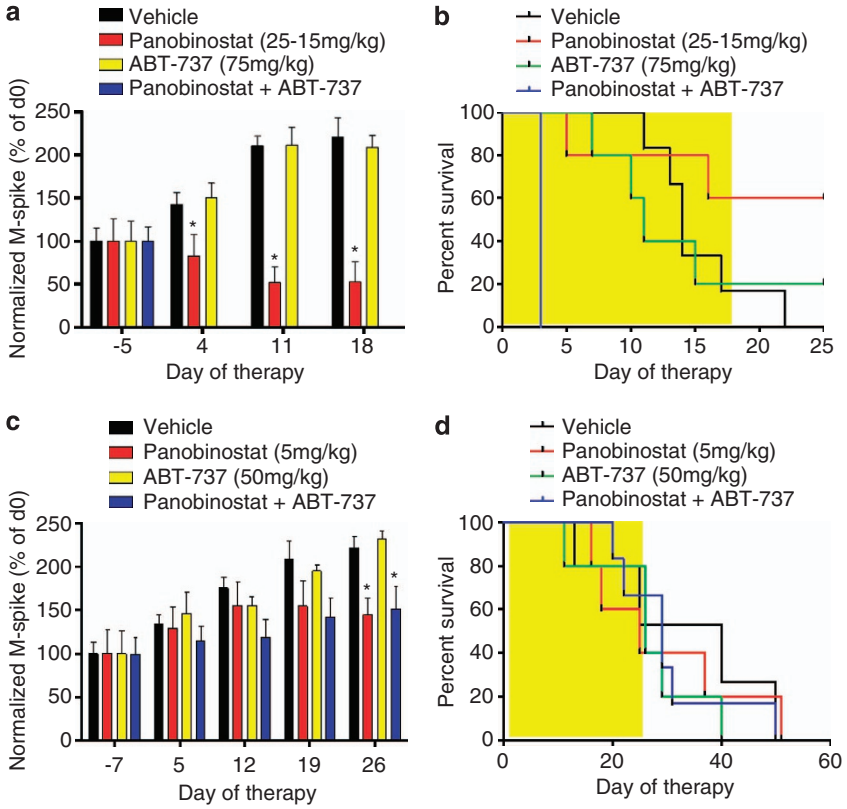

Figure 6 *In vivo* treatment of C57BL/6 mice bearing Vk*MYC MM reveals lack of therapeutic activity when panobinostat is combined with ABT-737 above that of panobinostat treatment alone. (**a**) Single-agent therapy consisting of vehicle (D5W), high-dose panobinostat (25 mg/kg days 1–4, 15 mg/kg remainder, 5 days per week), ABT-737 (75 mg/kg, 5 days per week) or the combination of both agents in mice bearing Vk*MYC MM. Normalized M-spike data over the 18 days of treatment. (**b**) Survival of mice treated with vehicle (D5W, $n=6$), panobinostat ($n=5$), ABT-737 ($n=5$) or the combination of both agents ($n=6$). (**c**) Mice bearing Vk*MYC MM were then treated with lower doses of both agents as follows: vehicle ($n=5$); panobinostat (5 mg/kg, 5 days per week, $n=5$); ABT-737 (50 mg/kg, two times daily, $n=5$); or the combination of both agents ($n=6$), for 4 weeks. Results are depicted as normalized M-spike over the 26 days of treatment, and (**d**) survival of mice treated with the lower doses of both agents, alone and in combination. *$P<0.05$ *versus* vehicle

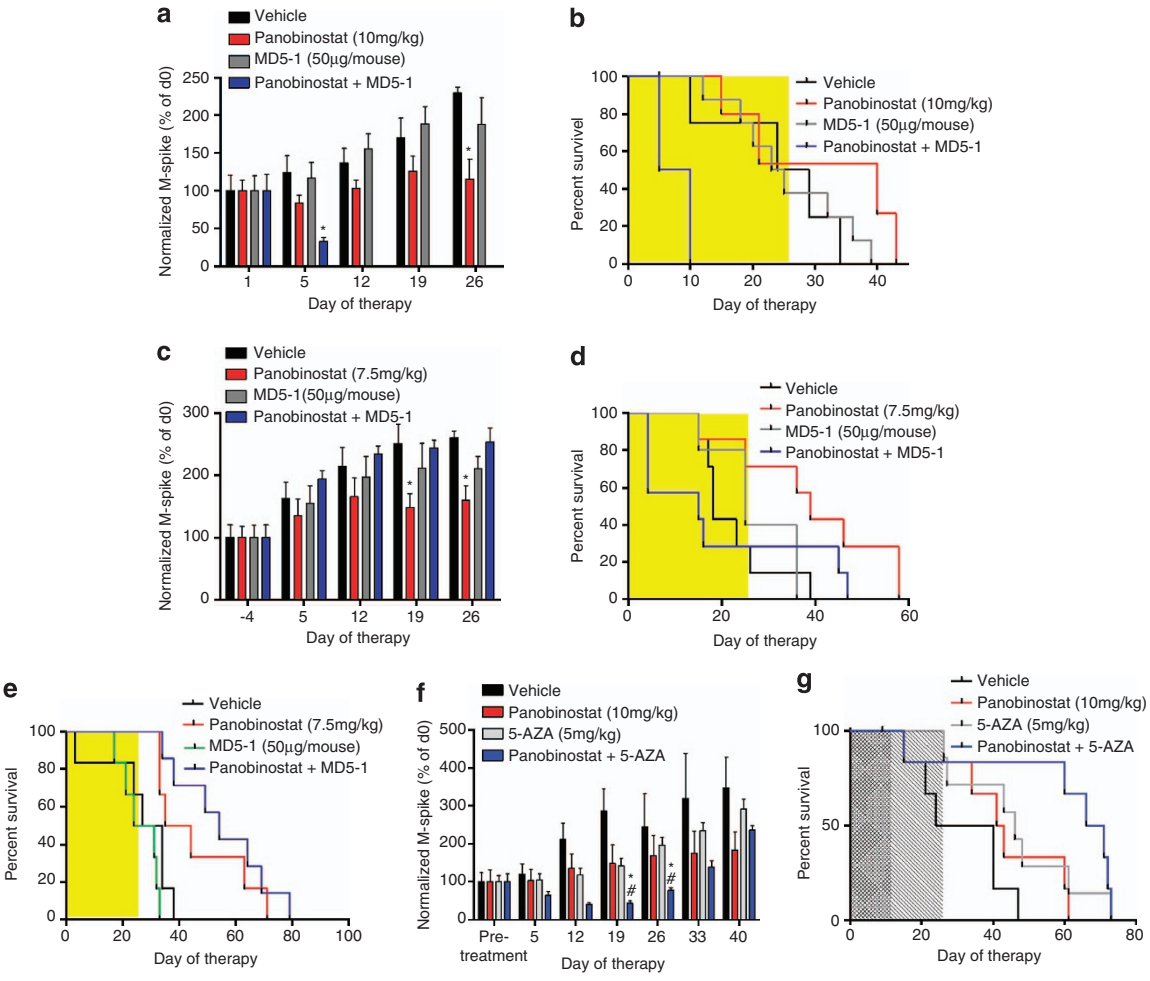

Figure 7 *In vivo* treatment consisting of panobinostat in combination with MD5-1 is not well tolerated and does not enhance survival of C57BL/6 mice bearing Vk*MYC MM over single-agent panobinostat treatment alone, whereas its combination with 5-AZA provides significant benefit. (**a**) Normalized M-spike of mice bearing Vk*MYC MM treated as follows: vehicle (D5W ± control antibody UC81B9, $n=8$); panobinostat (10 mg/kg, $n=6$); MD5-1 (50 μg per mouse; days 1, 4, 8, 12; $n=8$); or the combination of both agents ($n=8$). $^{*}P<0.05$ *versus* vehicle. (**b**) Survival of mice treated as per 7A, (**c**) normalized M-spike of mice bearing Vk*MYC MM treated as follows: vehicle (D5W, $n=7$); panobinostat (7.5 mg/kg, $n=7$); MD5-1 (50 μg per mouse; days 2, 5, 9, 12; $n=6$); or the combination of both agents ($n=7$); (**d**) survival of mice treated as per (**c**); (**e**) absence of on-target MD5-1-mediated toxicity by treatment of C57BL/6.DR5 KO mice bearing Vk*MYC tumor with panobinostat and MD5-1 combination therapy leads to significant increases in survival. Mice were treated as follows: vehicle (D5W ± control antibody UC81B9, $n=6$); panobinostat (7.5 mg/kg, $n=6$); MD5-1 (50μg per mouse, days 2, 5, 9, 12; $n=6$); or the combination of both agents ($n=7$); (**f**) normalized M-spike of mice bearing Vk*MYC MM treated as follows: vehicle (D5W, $n=6$), panobinostat (10 mg/kg, $n=6$), 5-AZA (5 mg/kg, $n=7$) and the combination of both agents ($n=7$). (**g**) Survival of mice treated as per (**f**). $^{*}P<0.05$ *versus* vehicle and $^{\#}P<0.05$ *versus* initial (pretreatment) SPEP

cell pellets were lysed (Triton X-100-based buffer) and protein concentration assessed.[53] Samples (20–40 μg) run into an SDS-PAGE gel (8–12%), wet transferred onto Immobilin P membrane (Millipore) and blocked (1 h, 5% skim milk). Primary antibodies were prepared in 5% skim milk in Tris-buffered saline with Tween (TBS-T) as follows: anti-acetylated histone H3, anti-Bcl-2, anti-Bcl-X_L, anti-Bcl-w, anti-Bcl-A1, anti-Mcl-1 and anti-cFLIP at 1/1000. β-Actin or α-tubulin (1/2000) were used as loading controls. Primary antibodies were incubated overnight at 4 °C. Secondary antibodies were prepared in 5% skim milk in TBS-T and incubated for 1 h at room temperature. Membranes were exposed to film after the addition of ECL (GE Healthcare, Melbourne, VIC, Australia). For assessment of c-FLIP mRNA expression, total RNA was obtained from cell pellets using Qiagen RNeasy mini kits (Qiagen, Doncaster, VIC, Australia) and reverse transcribed using M-MLV Reverse transcriptase (RNase H Minus, Point mutant) and random primers (Promega, Madison, WI, USA). Quantitative real-time polymerase chain reaction was undertaken using SYBR green fluorescent nucleic acid stain (Invitrogen, Mulgrave, VIC, Australia) and the following primers (Fwd: 5′-TGCCTCTCCCAGAAACTGAGA-3′; Rev: 5′-CCA ATCATACATGTAGCCATTGAGT-3′) in an ABI7900HT (Applied Biosystems, Mulgrave, VIC, Australia).

Oncomine database search. Microarray data sets were assessed using Oncomine Cancer Profiling Database (http: //www.oncomine.org/). The expression of prosurvival *Bcl-2* genes in human JJN3, OPM-2, RPMI-8226 and U266 cells were obtained through Oncomine software 4.4.3 (Compendia Bioscience, Ann Arbor, MI, USA).

RNA sequencing. JJN3 and U266 cells were treated with panobinostat (4 h), 5-AZA (24 + 4 h) or the combination of both agents (24 + 4 h) at doses deemed to be synergistic (Figure 4b), harvested and RNA extracted as described. Fifty base pair paired-end reads were generated on an Illumina Hiseq. Reads were quality checked by FastQC and trimmed if necessary for low base quality or adaptor, and then mapped to the human reference genome (GRCh37) using Tophat2 v.2.0.8b (PMID: 23618408) with maximum number of multiple hits set to 1 and using the option to map first to the reference

transcriptome (Ensembl v.69). Counts per gene were obtained using HTSeq v.0.5.3p9 with mode intersection-nonempty (http: //www-huber.embl.de/users/anders/HTSeq/doc/overview.html/). The limma-voom method was used to identify genes differentially expressed between each drug (or combination) and the vehicle control using a FDR threshold <0.05 (http: //www.statsci.org/smyth/pubs/VoomTechReport.pdf/).

Gene set testing was performed using CAMERA[40] and the MSigDB v.3.1 C2 curated gene sets collection. The genes in the RNA-seq data set were mapped to the Entrez IDs in the gene sets by first mapping the RNA-seq Ensembl gene IDs to Entrez IDs. Gene sets that contained fewer than 15 genes were excluded. After running CAMERA, two-sided *P*-values of <0.05 were applied to identify statistically significant signatures.

Analysis of DR-4 and DR-5 expression by FACS. Cell lines were suspended at $1 \times 10^6/100\,\mu$l in PBS and stained with anti-hDR-4, DR-5 (1/20) or isotype control for 30 min on ice. Cells were washed in PBS, stained with anti-IgG-PE (1/200) for 30 min on ice, washed and analyzed on a Canto II (Becton Dickinson) flow cytometer.

Therapeutic assessment of antitumor agents. Recipient C57BL/6 mice (typically $n=10$ per intended treatment cohort) were injected intravenously with Vk*MYC MM cells ($2–5 \times 10^5$ per mouse) following conditioning with two fractions of 3 Gy irradiation. Mice were monitored for the onset of paraproteinemia by periodic serum protein electrophoresis (SPEP). Mice with established paraproteinemia ($>5\%$ of total protein) were grouped based on approximately equal mean paraprotein levels and randomly assigned to treatment groups. For determination of 'on-target' toxicity in response to MD5-1 treatment, Vk*MYC tumor was transplanted into C57BL/6.DR5$^{-/-}$ mice.

Mice bearing Vk*MYC tumor were treated for 4 weeks as follows: (a) vehicle (D5W, 200 μl daily), panobinostat (25 mg/kg days 1–4, then 15 mg/kg 5 days per week); (b) panobinostat (10, 7.5 or 5 mg/kg, 5 days per week, intraperitoneally), ABT-737 (75 or 50 mg/kg, intraperitoneally, two times daily), or the combination of both agents; (c) monoclonal control antibody (UC8-1B9, 50 μg per mouse) in D5W, panobinostat (10 g or 7.5 mg/kg), anti-mouse agonistic anti-TRAIL antibody MD5-1 (50 μg per mouse or 25 μg per mouse) or the combination of both agents; and (d) panobinostat (10 mg/kg 5days per week, intraperitoneally), 5-AZA (5 mg/kg, two times daily, 12 days, intraperitoneally) or the combination of both agents. Therapeutic efficacy was assessed by serial SPEP obtained by retro-orbital sampling or tail grazing. Mice were culled by cervical dislocation at predetermined end points, including hind limb paralysis, cachexia and hunching.

Mice were maintained under specific pathogen-free conditions and used in accordance with the institutional guidelines of the Peter MacCallum Cancer Centre. Animal care was provided in accordance with the procedures outlined in the National Institutes of Health Guide for the Care and Use of Laboratory Animals.

Assessment of DR-5 expression on Vk*MYC tumor. Bone marrow suspensions from mice bearing transplanted Vk*MYC tumor were washed (2% FBS in PBS), red cell lysed and stained with anti-mB220-FITC (1/400), anti-mCD138-PE (1/500), anti-IgD-Pacblue (1/300), biotin-labeled anti-mDR5 (1/500) or isotype control (Armenian hamster IgG, 1/500). Plates were set on ice for 30 min, washed and stained with streptavidin-labeled secondary antibody conjugated to APC on ice for 30 min. Following two washes, cells were resuspended in PBS containing fluorogold (1/3000) and assessed for DR5 expression using an LSR II flow cytometer (Becton Dickinson).

Statistics. The sensitivity of MM cell lines to tested agents were compared using GraphPad software (Prism, GraphPad Software Inc., La Jolla, CA, USA). Combination drug experiments were assessed for synergy, additivity or antagonism using Calcusyn (Biosoft, Cambridge, UK), which uses the median-effect equation of Chou and Talalay.[54] Statistical analyses of *in vivo* therapy assays were performed using one-way analysis of variances (ANOVA) with *post hoc* tests. Median survival between treatment groups were compared using Kaplan–Meier curves and the GraphPad software. Significance was assumed with $P<0.05$.

Conflict of Interest

GMM, ML, MD, JS, JE, KB, EV and DF declare no conflict of interest. The laboratory of RWJ receives research funding from Novartis for studies involving panobinostat. PA is an employee of Novartis. PLB and MC hold intellectual property in Vk*MYC mice.

Acknowledgements. We thank Dr Hideo Yagita for the provision of MD5-1. GMM was supported by funding from the National Health and Medical Research Council (NHMRC) of Australia. JS was supported by funding from the Leukaemia Foundation of Australia and the Co-operative Research Centre for Biomedical Imaging Development. RWJ is a Principal Research Fellow of the NHMRC of Australia and supported by NHMRC Program and Project Grants, the Susan G Komen Breast Cancer Foundation, Cancer Council Victoria, The Leukaemia Foundation of Australia, Victorian Breast Cancer Research Consortium and the Victorian Cancer Agency. ML is supported by the Leukaemia Foundation of Australia. This work was supported by National Institutes of Health Grant AG20686, National Cancer Institute Grant CA136671 (PLB) and by the Multiple Myeloma Research Foundation (MC).

1. Kyle RA, Buadi F, Rajkumar SV. Management of monoclonal gammopathy of undetermined significance (MGUS) and smoldering multiple myeloma (SMM). *Oncology (Williston Park)* 2011; **25**: 578–586.
2. Kyle RA, Rajkumar SV. Multiple myeloma. *N Engl J Med* 2004; **351**: 1860–1873.
3. Chesi M, Robbiani DF, Sebag M, Chng WJ, Affer M, Tiedemann R *et al.* AID-dependent activation of a MYC transgene induces multiple myeloma in a conditional mouse model of post-germinal center malignancies. *Cancer Cell* 2008; **13**: 167–180.
4. Kyle RA, Rajkumar SV. Criteria for diagnosis, staging, risk stratification and response assessment of multiple myeloma. *Leukemia* 2009; **23**: 3–9.
5. Azab AK, Runnels JM, Pitsillides C, Moreau AS, Azab F, Leleu X *et al.* CXCR4 inhibitor AMD3100 disrupts the interaction of multiple myeloma cells with the bone marrow microenvironment and enhances their sensitivity to therapy. *Blood* 2009; **113**: 4341–4351.
6. Khong T, Sharkey J, Spencer A. The effect of azacitidine on interleukin-6 signaling and nuclear factor-kappaB activation and its *in vitro* and *in vivo* activity against multiple myeloma. *Haematologica* 2008; **93**: 860–869.
7. Utecht KN, Kolesar J. Bortezomib: a novel chemotherapeutic agent for hematologic malignancies. *Am J Health Syst Pharm* 2008; **65**: 1221–1231.
8. Atadja PW. HDAC inhibitors and cancer therapy. *Prog Drug Res* 2011; **67**: 175–195.
9. Bolden JE, Peart MJ, Johnstone RW. Anticancer activities of histone deacetylase inhibitors. *Nat Rev Drug Discov* 2006; **5**: 769–784.
10. Khan O, La Thangue NB. HDAC inhibitors in cancer biology: emerging mechanisms and clinical applications. *Immunol Cell Biol* 2012; **90**: 85–94.
11. Fantin V, Richon VM. Mechansims of resistance to histone deacetylase inhibitors and their therapeutic implications. *Clin Cancer Res* 2007; **13**: 7237–7242.
12. Hacker S, Dittrich A, Mohr A, Schweitzer T, Rutkowski S, Krauss J *et al.* Histone deacetylase inhibitors cooperate with IFN-gamma to restore caspase-8 expression and overcome TRAIL resistance in cancers with silencing of caspase-8. *Oncogene* 2009; **28**: 3097–3110.
13. Rasheed W, Bishton M, Johnstone R, Prince M. Histone deacetylase inhibitors in lymphoma and solid malignancies. *Expert Rev Anticancer Ther* 2008; **8**: 413–432.
14. Vanoosten RL, Moore JM, Ludwig AT, Griffith TS. Depsipeptide (FR901228) enhances the cytotoxic activity of TRAIL by redistributing TRAIL receptor to membrane lipid rafts. *Mol Ther* 2005; **11**: 542–552.
15. Atadja P. Development of the pan-DAC inhibitor panobinostat (LBH589): successes and challenges. *Cancer Lett* 2009; **280**: 233–241.
16. Maiso P, Carvajal-Vergara X, Ocio EM, Lopez-Perez R, Mateo G, Gutierrez N *et al.* The histone deacetylase inhibitor LBH589 is a potent antimyeloma agent that overcomes drug resistance. *Cancer Res* 2006; **66**: 5781–5789.
17. Martin BP, Frew AJ, Bots M, Fox S, Long F, Takeda K *et al.* Antitumor activities and on-target toxicities mediated by a TRAIL receptor agonist following cotreatment with panobinostat. *Int J Cancer* 2011; **128**: 2735–2747.
18. Buchwald M, Kramer OH, Heinzel T. HDACi-targets beyond chromatin. *Cancer Lett* 2009; **280**: 160–167.
19. Chipuk JE, Green DR. How do BCL-2 proteins induce mitochondrial outer membrane permeabilization? *Trends Cell Biol* 2008; **18**: 157–164.
20. Chipuk JE, Moldoveanu T, Llambi F, Parsons MJ, Green DR. The BCL-2 family reunion. *Molecular Cell* 2010; **37**: 299–310.
21. Konopleva M, Contractor R, Tsao T, Samudio I, Ruvolo PP, Kitada S *et al.* Mechanisms of apoptosis sensitivity and resistance to the BH3 mimetic ABT-737 in acute myeloid leukemia. *Cancer Cell* 2006; **10**: 375–388.
22. Lessene G, Czabotar PE, Colman PM. BCL-2 family antagonists for cancer therapy. *Nat Rev Drug Discov* 2008; **7**: 989–1000.
23. Letai A. Pharmacological manipulation of Bcl-2 family members to control cell death. *J Clin Invest* 2005; **115**: 2648–2655.
24. Letai A. BCL-2: found bound and drugged! *Trends Mol Med* 2005; **11**: 442–444.

25. Oltersdorf T, Elmore SW, Shoemaker AR, Armstrong RC, Augeri DJ, Belli BA *et al.* An inhibitor of Bcl-2 family proteins induces regression of solid tumours. *Nature* 2005; **435**: 677–681.
26. Trudel S, Stewart AK, Li Z, Shu Y, Liang SB, Trieu Y *et al.* The Bcl-2 family protein inhibitor, ABT-737, has substantial antimyeloma activity and shows synergistic effect with dexamethasone and melphalan. *Clin Cancer Res* 2007; **13**(Part 1): 621–629.
27. Johnstone RW, Frew AJ, Smyth MJ. The TRAIL apoptotic pathway in cancer onset, progression and therapy. *Nat Rev Cancer* 2008; **8**: 782–798.
28. Wang S. The promise of cancer therapeutics targeting the TNF-related apoptosis-inducing ligand and TRAIL receptor pathway. *Oncogene* 2008; **27**: 6207–6215.
29. Frew AJ, Johnstone RW, Bolden JE. Enhancing the apoptotic and therapeutic effects of HDAC inhibitors. *Cancer Lett* 2009; **280**: 125–133.
30. Frew AJ, Lindemann RK, Martin BP, Clarke CJ, Sharkey J, Anthony DA *et al.* Combination therapy of established cancer using a histone deacetylase inhibitor and a TRAIL receptor agonist. *Proc Natl Acad Sci USA* 2008; **105**: 11317–11322.
31. Whitecross KF, Alsop AE, Cluse LA, Wiegmans A, Banks K-M, Coomans C *et al.* Defining the target specificity of ABT-737 and synergistic antitumor activities in combination with histone deacetylase inhibitors. *Blood* 2009; **113**: 1982–1991.
32. Wiegmans AP, Alsop A, Bots M, Cluse LA, Williams SP, Banks K-M *et al.* Deciphering the molecular events necessary for synergistic tumor cell apoptosis mediated by the histone deacetylase inhibitor vorinostat and the BH3 mimetic ABT-737. *Cancer Res* 2011; **71**: 3603–3615.
33. Smith EM, Boyd K, Davies FE. The potential role of epigenetic therapy in multiple myeloma. *Br J Haematol* 2010; **148**: 702–713.
34. Nojima M, Maruyama R, Yasui H, Suzuki H, Maruyama Y, Tarasawa I *et al.* Genomic screening for genes silenced by DNA methylation revealed an association between RASD1 inactivation and dexamethasone resistance in multiple myeloma. *Clin Cancer Res* 2009; **15**: 4356–4364.
35. Chesi M, Matthews GM, Garbitt VM, Palmer SE, Shortt J, Lefebure M *et al.* Drug response in a genetically engineered mouse model of multiple myeloma is predictive of clinical efficacy. *Blood* 2012; **120**: 376–385.
36. Chng WJ, Huang GF, Chung TH, Ng SB, Gonzalez-Paz N, Troska-Price T *et al.* Clinical and biological implications of MYC activation: a common difference between MGUS and newly diagnosed multiple myeloma. *Leukemia* 2011; **25**: 1026–1035.
37. Ellis L, Bots M, Lindemann RK, Bolden JE, Newbold A, Cluse LA *et al.* The histone deacetylase inhibitors LAQ824 and LBH589 do not require death receptor signaling or a functional apoptosome to mediate tumor cell death or therapeutic efficacy. *Blood* 2009; **114**: 380–393.
38. Lindemann RK, Newbold A, Whitecross KF, Cluse LA, Frew AJ, Ellis L *et al.* Analysis of the apoptotic and therapeutic activities of histone deacetylase inhibitors by using a mouse model of B cell lymphoma. *Proc Natl Acad Sci USA* 2007; **104**: 8071–8076.
39. Ruefli AA, Ausserlechner MJ, Bernhard D, Sutton VR, Tainton KM, Kofler R *et al.* The histone deacetylase inhibitor and chemotherapeutic agent suberoylanilide hydroxamic acid (SAHA) induces a cell-death pathway characterized by cleavage of Bid and production of reactive oxygen species. *Proc Natl Acad Sci USA* 2001; **98**: 10833–10838.
40. Wu D, Smyth GK. Camera: a competitive gene set test accounting for inter-gene correlation. *Nucleic Acids Res* 2012; **40**: e133.
41. Deleu S, Lemaire M, Arts J, Menu E, Van Valckenborgh E, Vande Broek I *et al.* Bortezomib alone or in combination with the histone deacetylase inhibitor JNJ-26481585: effect on myeloma bone disease in the 5T2MM murine model of myeloma. *Cancer Res* 2009; **69**: 5307–5311.
42. Feng R, Oton A, Mapara MY, Anderson G, Belani C, Lentzsch S. The histone deacetylase inhibitor, PXD101, potentiates bortezomib-induced anti-multiple myeloma effect by induction of oxidative stress and DNA damage. *Br J Haematol* 2007; **139**: 385–397.
43. Mitsiades N, Mitsiades CS, Richardson PG, McMullan C, Poulaki V, Fanourakis G *et al.* Molecular sequelae of histone deacetylase inhibition in human malignant B cells. *Blood* 2003; **101**: 4055–4062.
44. Zhang L, Fang B. Mechanisms of resistance to TRAIL-induced apoptosis in cancer. *Cancer Gene Ther* 2004; **12**: 228–237.
45. Guo F, Sigua C, Tao J, Bali P, George P, Li Y *et al.* Cotreatment with histone deacetylase inhibitor LAQ824 enhances Apo-2L/tumor necrosis factor-related apoptosis inducing ligand-induced death inducing signaling complex activity and apoptosis of human acute leukemia cells. *Cancer Res* 2004; **64**: 2580–2589.
46. Kauh J, Fan S, Xia M, Yue P, Yang L, Khuri FR *et al.* c-FLIP degradation mediates sensitization of pancreatic cancer cells to TRAIL-induced apoptosis by the histone deacetylase inhibitor LBH589. *PLoS One* 2010; **5**: e10376.
47. Perez LE, Parquet N, Shain K, Nimmanapalli R, Alsina M, Anasetti C *et al.* Bone marrow stroma confers resistance to Apo2 ligand/TRAIL in multiple myeloma in part by regulating c-FLIP. *J Immunol* 2008; **180**: 1545–1555.
48. Gomez-Benito M, Martinez-Lorenzo MJ, Anel A, Marzo I, Naval J. Membrane expression of DR4, DR5 and caspase-8 levels, but not Mcl-1, determine sensitivity of human myeloma cells to Apo2L/TRAIL. *Exp Cell Res* 2007; **313**: 2378–2388.
49. Brennan SK, Matsui W. Cancer stem cells: controversies in multiple myeloma. *J Mol Med (Berl)* 2009; **87**: 1079–1085.
50. Labrinidis A, Diamond P, Martin S, Hay S, Liapis V, Zinonos I *et al.* Apo2L/TRAIL inhibits tumor growth and bone destruction in a murine model of multiple myeloma. *Clin Cancer Res* 2009; **15**: 1998–2009.
51. Vogler M, Butterworth M, Majid A, Walewska RJ, Sun XM, Dyer MJ *et al.* Concurrent up-regulation of BCL-XL and BCL2A1 induces approximately 1000-fold resistance to ABT-737 in chronic lymphocytic leukemia. *Blood* 2009; **113**: 4403–4413.
52. Vogler M, Dinsdale D, Dyer MJS, Cohen GM. Bcl-2 inhibitors: small molecules with a big impact on cancer therapy. *Cell Death Differ* 2008; **16**: 360–367.
53. Bradford MM. A rapid and sensitive method for the quantitation of microgram quantities of protein utilizing the principle of protein-dye binding. *Anal Biochem* 1976; **72**: 248–254.
54. Chou TC. Drug combination studies and their synergy quantification using the Chou–Talalay method. *Cancer Res* 2010; **70**: 440–446.

Supplementary Information accompanies this paper on Cell Death and Disease website (http://www.nature.com/cddis)